Sub-Optimal Control of Unsteady Separation in a Channel

K. W. Cassel*, C. Sardesai*, S. Braun† and A. I. Ruban‡

*MMAE Department, Illinois Institute of Technology, Chicago, Illinois, USA (cassel@iit.edu).
†Institute of FMHT, Vienna University of Technology, Vienna, Austria.
‡School of Mathematics, University of Manchester, Manchester, UK.

Abstract. Incompressible flow through a two-dimensional channel with localized suction from the upper surface is considered as a framework within which to consider the control of unsteady separation within the context of boundary-layer theory. The strength of the adverse pressure gradient, which gives rise to the unsteady separation, is determined by the proportion of the incoming flow into the channel that exits through the suction slot, providing a means by which to adjust the intensity of the unsteady separation process. Control is implemented through either a body force throughout the boundary layer or boundary conditions at the lower surface where the unsteady separation takes place. The control objective is to suppress the onset of unsteady separation by minimizing a cost functional that retards the separation process while minimizing the energy input required to accomplish the control. In the present investigation, sub-optimal control is considered in which the control, *i.e.* adjoint, equation is solved in a quasi-steady manner as the unsteady boundary-layer equations evolve in time.

Key words: channel flow, boundary layer, unsteady separation, sub-optimal control.

1. Introduction

1.1. Background

Unsteady separation plays a pivotal role in a number of important high-Reynolds-number applications in which an adverse pressure gradient acts on a boundary layer (see Doligalski, Smith & Walker 1994 for a review). The adverse pressure gradient may be a result of the surface geometry, such as the leading edge of an airfoil at angle of attack, or it may result from the presence of a vortex above the surface, such as coherent structures in turbulent boundary layers or the dynamic-stall vortex above an airfoil or helicopter blade. Alternatively, the adverse pressure gradient may arise upstream of surface-mounted obstacles or in the vicinity of pipe or vessel branchings. Unsteady separation begins as a recirculation region forms within the boundary layer owing to the adverse pressure gradient, and it culminates in an abrupt ejection of near-wall vorticity into the outer flow (see Obabko & Cassel 2002b, and the references therein). In fact, the unsteady boundary-layer equations become singular under such conditions (Van Dommelen & Shen 1980, Peridier *et al.* 1991). Although the unsteady separation event itself is localized spatially and occurs over a very short time scale, it often has dramatic global consequences for the flows in which it occurs. For example, the need to avoid dynamic stall on helicopter blades and airfoils limits their range of performance and maneuverability.

The fact that unsteady separation is a small-scale, localized event that typically has global consequences makes it an ideal candidate for flow control. The ability to *control* unsteady separation, *i.e.* to eliminate it in situations where it is undesirable or induce it in situations where it would be beneficial, could provide a long ‘lever arm’ with which to modify flows in certain applications toward a more desirable state with minimum energy input required. Elimination of unsteady separation could increase the performance of aircraft and rotorcraft by delaying dynamics stall on pitching airfoils, allowing for shortening of the inlet nozzles of aircraft engines or increasing performance of the compressor and turbine stages of turbomachinery. Inducing unsteady separation, on the other hand, could dramatically increase fluid and/or thermal mixing in applications where that would be desirable.

Attempts have been made to control unsteady separation using moving walls, blowing or suction, and buoyancy forces (see, for example, Alrefai & Acharya 1996, Degani *et al.* 1998, Cassel 2001, Obabko & Cassel 2002a). The typical approach to controlling phenomena, such at turbulence or separation, in fluid dynamical contexts is to choose or develop an actuator or methodology that modifies the flow field in a particular manner, and then test the approach on a prescribed problem by comparing the control and the no-control behavior to determine the effectiveness of the control strategy. This approach requires a detailed understanding of the underlying flow, and all too often it involves measures of effectiveness that are too qualitative and subjective, appealing to an imprecise notion of how the flow should behave. As a result, it is difficult to quantitatively compare the effectiveness of various control schemes with regard to their effectiveness and energy input requirements. This traditional approach to flow control may work reasonably well for a particular application or problem, while leaving the questions of "whether the effort expended in controlling the flow is justified by the benefits yielded" and "whether the approach is the *best* means of controlling the flow" largely unanswered.

Optimal control theory, based on variational methods, offers a more formal means by which to determine the *best* approach to meeting a prescribed control objective in a particular flow environment. Flow control based on optimal control theory has been applied successfully to drag reduction in turbulent channel flow (see Bewley *et al.* 2001, and the references therein) and the flow past a circular cylinder (Min & Choi 1999). This approach requires a clearly articulated prescription of the controlled flow conditions, i.e. what is meant by *optimal* control, through specification of a cost functional to be minimized. Minimization of the cost functional subject to the constraint that the governing equations are satisfied leads to the optimal approach to affect the desired control. This provides an upper bound on the potential for flow control in a given application. In addition, the optimal control results provide practical guidance to those developing and testing sensors and actuators, such as 1) what type of sensors are required to determine the state of the flow, 2) what type of actuator most closely emulates the optimal control strategy, 3) what control authority, i.e. energy input, is required for the intended application, 4) where should the actuators be placed, and 5) when should they be turned on? Ultimately, the variational approach could be incorporated into a feedback control loop to determine the optimal control input for an actual flow state in order to bring about a more desirable controlled flow at a later time.

1.2. Channel Flow with Suction

An ideal model problem in which to investigate unsteady separation and its control is the flow through a channel with a suction slot located on the upper surface. The presence of the suction slot gives rise to an adverse pressure gradient immediately below it on the lower wall of the channel, which is the primary region of interest in the present study. The magnitude of the suction determines the severity of the adverse pressure gradient and the concomitant response of the boundary layer along the lower wall. This problem is somewhat simpler than previous model problems in which unsteady separation has been considered, see for example the vortex above a wall (Peridier *et al.* 1991, Cassel 2000 and Obabko & Cassel 2002b), and it allows for varying of the magnitude of the adverse pressure gradient in a straightforward manner.

A schematic of the channel problem is shown in figure 1. Solutions for the two-dimensional, incompressible flow through the channel subject to suction from the upper surface are considered, where Q_i is the inlet volume flow rate, Q_o is the flow rate at the outlet of the channel, and Q_s is the flow rate through the suction slot, such that $Q_o = Q_i - Q_s$. The inlet flow is uniform of velocity U, and the height of the channel is H. The velocity through the suction slot of width b is also uniform with speed S. The strength of the adverse pressure gradient is determined by the suction ratio $\alpha = Q_s/Q_i$, which gives the relative amount of inlet flow that exits through the suction slot; thus, $Q_o = (1-\alpha)Q_i$. Note that although this flow is similar to that investigated by Pauley *et al.* (1990) and Alam & Sandham (2000), a Blasius inlet profile was used with a slip condition, *i.e.* $u = 1$, along the upper wall in the referenced investigations in order to more closely emulate an external flow.

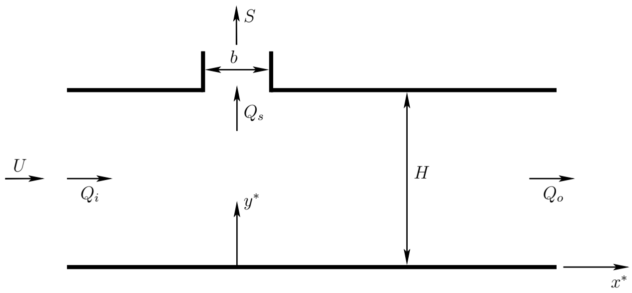

Figure 1. Schematic of the channel with suction slot.

In order to illustrate some of the overall flow features and the range of possible behaviors, results are given for computations of the full unsteady, two-dimensional Navier-Stokes equations for this model problem. These solutions reveal that for certain ranges of the Reynolds number ($Re = UH/\nu$) and suction ratio (α) there are various regimes involving steady separation, unsteady separation and/or shedding along the lower wall beneath the suction slot. Two examples are shown in figures 2 and 3. The first case shown in figure 2 with $Re = 5,000$ and $\alpha = 0.08$ results in the formation of a steady recirculation region along the lower wall after some period of time. The second case shown in figure 3 with $Re = 10,000$ and $\alpha = 0.30$ involves vortex shedding along the lower surface with corresponding unsteady separation events.

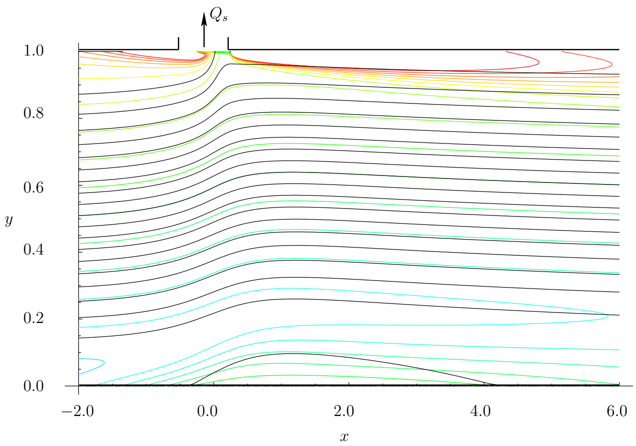

Figure 2. Steady Navier-Stokes solution of channel flow with suction for $Re = 5,000$ and $\alpha = 0.08$.

2. Unsteady Boundary-Layer Control

Optimal control theory is used in this investigation to evaluate different approaches to controlling, in this case suppressing, unsteady separation in the channel flow with suction within the context of the unsteady boundary-layer formulation. The various flow control strategies can be classified as those that either seek to modify the flow using a body force throughout the domain, e.g. through plasma actuators or a Lorentz force, or changes in boundary conditions, e.g. blowing or suction. Using the optimal control approach, it is not necessary to decide on a specific method of actuation, only on whether it is *domain* or *boundary* based. The next section details the unsteady boundary-layer formulation, *i.e.* the state equations, that forms the basis for the control algorithm, which is outlined in the following section.

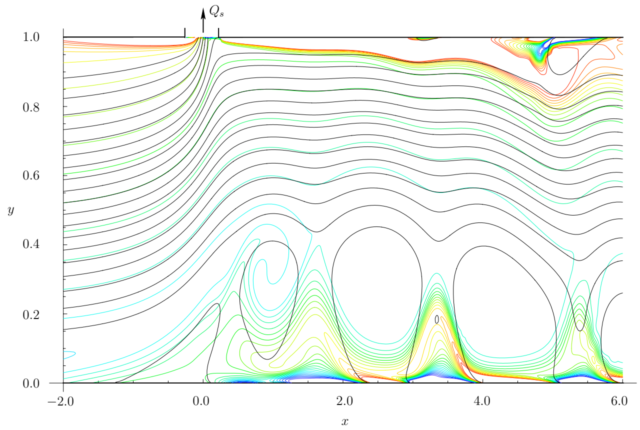

Figure 3. Navier-Stokes solution of channel flow with suction at $t = 25$ for $Re = 10,000$ and $\alpha = 0.30$.

2.1. Unsteady Boundary-Layer Formulation

Although the overall flow within the channel is governed by the unsteady, two-dimensional Navier-Stokes equations, it is advantageous to utilize a reduced model, in this case the unsteady boundary-layer equations, as the basis for investigation of control of unsteady separation along the lower surface of the channel. Use of a reduced model, as compared to the full Navier-Stokes equations, results in a control problem that is much more amenable to solution computationally. Specifically, rather than two momentum equations as in the Navier-Stokes equations, only one momentum equation is present in the boundary-layer formulation. In addition, the boundary-layer formulation governs the early stages of the unsteady separation process at high Reynolds numbers during which it is most sensitive to control, resulting in the most effective means by which to suppress unsteady separation with the least amount of control input.

The unsteady, two-dimensional Navier-Stokes equations with body force terms X^* and Y^* are

$$\frac{\partial u^*}{\partial t^*} + u^* \frac{\partial u^*}{\partial x^*} + v^* \frac{\partial u^*}{\partial y^*} = -\frac{1}{\rho}\frac{\partial p^*}{\partial x^*} + \nu \left[\frac{\partial^2 u^*}{\partial x^{*2}} + \frac{\partial^2 u^*}{\partial y^{*2}}\right] + X^*, \tag{1}$$

$$\frac{\partial v^*}{\partial t^*} + u^* \frac{\partial v^*}{\partial x^*} + v^* \frac{\partial v^*}{\partial y^*} = -\frac{1}{\rho}\frac{\partial p^*}{\partial y^*} + \nu \left[\frac{\partial^2 v^*}{\partial x^{*2}} + \frac{\partial^2 v^*}{\partial y^{*2}}\right] + Y^*, \tag{2}$$

$$\frac{\partial u^*}{\partial x^*} + \frac{\partial v^*}{\partial y^*} = 0. \tag{3}$$

We non-dimensionalize and introduce the boundary-layer scales for the boundary layer along the lower wall as follows

$$x = \frac{x^*}{H}, \quad y = \frac{y^*}{H} Re^{1/2}, \quad t = \frac{t^* U}{H}, \quad u = \frac{u^*}{U}, \quad v = \frac{v^*}{U} Re^{1/2}, \quad p = \frac{p^*}{\rho U^2}, \quad (4)$$

where the Reynolds number is defined by $Re = UH/\nu$, and we take $Re \to \infty$. Substituting the scalings into the y-momentum equation (2) leads to $\partial p/\partial y = 0$ to leading order; therefore, $p = p(x)$ is prescribed by the outer inviscid flow and imposed vertically across the boundary layer. Substituting (4) into (1) and (3) gives the boundary-layer equations

$$\frac{\partial u}{\partial t} + u\frac{\partial u}{\partial x} + v\frac{\partial u}{\partial y} = -\frac{dp}{dx} + \frac{\partial^2 u}{\partial y^2} + X, \quad \frac{\partial u}{\partial x} + \frac{\partial v}{\partial y} = 0, \quad (5)$$

where the non-dimensional body force is $X = HX^*/U^2$. The initial conditions are

$$u(x, y, 0) = u_0(x, y), \quad v(x, y, 0) = v_0(x, y), \quad (6)$$

where $u_0(x, y)$ and $v_0(x, y)$ are specified, and the boundary conditions are

$$\begin{gathered} u(x, 0, t) = u_w(x, t), \quad u(x, \infty, t) = U_e(x), \quad u(\pm\infty, y, t) = u_\infty(y, t), \\ v(x, 0, t) = v_w(x, t), \quad v(\pm\infty, y, t) = v_\infty(y, t), \end{gathered} \quad (7)$$

where $u_\infty(y, t)$ and $v_\infty(y, t)$ are specified velocity profiles at upstream and downstream infinity, $u_w(x, t)$ and $v_w(x, t)$ are tangential and normal velocities, respectively, at the lower wall, and $U_e(x)$ is the prescribed external velocity at the outer edge of the boundary layer from the inviscid solution. Note that the normal body force term Y^* does not appear in the leading-order boundary-layer equations. The candidate control variables are the body force $X(x, y, t)$, which is a *domain*-based control mechanism, and the tangential and normal wall velocities $u_w(x, t)$ and $v_w(x, t)$, respectively, which are *boundary*-based control mechanisms.

The pressure gradient required for solution of the boundary-layer equations is obtained from the inviscid solution for the flow through the channel. The inviscid solution for the channel geometry with uniform suction may be obtained using the method of distributed singularities and images. The resulting streamwise velocity along the lower wall, which is the external velocity $U_e(x)$ at the outer edge of the boundary layer, is given by

$$U_e(x) = 1 - \frac{\alpha}{2} + \frac{\alpha}{2} \ln \left[\frac{\cosh(\frac{\pi}{2}(x - \frac{b}{2}))}{\cosh(\frac{\pi}{2}(x + \frac{b}{2}))} \right]. \quad (8)$$

Recall that $\alpha = Q_s/Q_i$ is the suction ratio, and b is the width of the suction slot, here taken as $b = 0.5$ for all cases. The corresponding pressure gradient along the lower wall required for equation (5) that is imposed across the boundary layer is obtained from equation (8) using the Bernoulli equation. The inviscid velocity and pressure gradient along the lower wall are shown in figure 4 for $\alpha = 0.10$, *i.e.* ten percent of the incoming fluid exits through the suction slot.

2.2. Optimal and Sub-Optimal Control

Proper selection of a cost functional, which ultimately defines what is meant by *optimal* control, requires a clear understanding of the physics of the flow to be controlled. For example, to minimize the drag on an object one would expect that a cost functional in which the drag is directly minimized would be the most effective. However, as shown by Min & Choi (1999) for the case of a circular cylinder and Bewley *et al.* (2001) for the case of a turbulent channel flow, this is often not the case as minimizing the *cause* of the drag often is more effective than minimizing the drag itself. This is particularly relevant in the present context for which the control objective is to suppress unsteady separation, which is not a quantity that can be minimized, but rather a phenomenon. Therefore, it is instead necessary to minimize a quantity that will consequently prevent unsteady separation, requiring intimate knowledge of the processes leading up to unsteady separation.

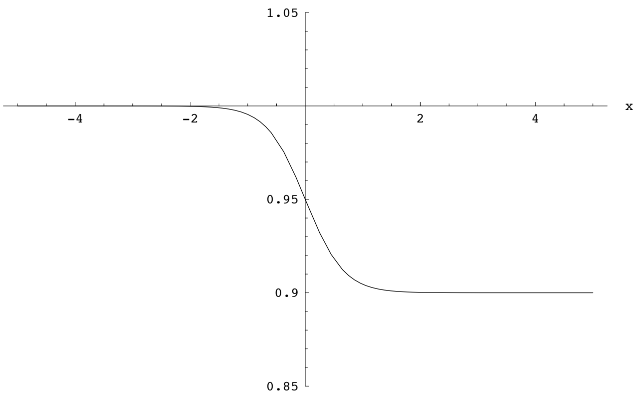

(a) Velocity distribution.

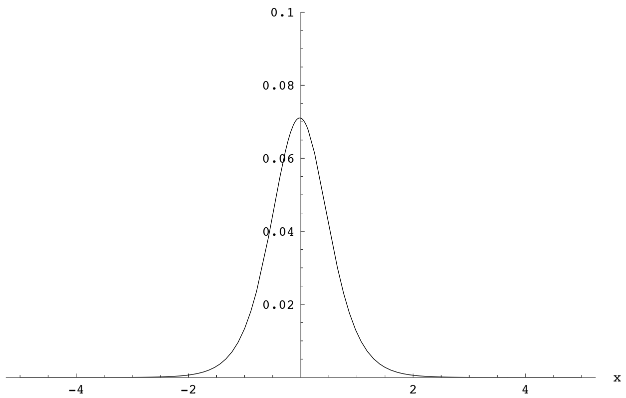

(b) Streamwise pressure gradient.

Figure 4. Inviscid solution along the lower wall for $\alpha = 0.10$.

Recall that the root cause of unsteady separation is an adverse pressure gradient acting upon the boundary layer. Therefore, what is being sought is a domain- or boundary-based control mechanism that will counteract the effects of the adverse pressure gradient on the boundary layer, thereby preventing unsteady separation. In the present case, the domain-based actuation would be due to some body force, and the boundary-based actuation would be due to the boundary conditions on velocity at the surface, *e.g.* blowing, suction or a moving wall.

Just as with the actuation methods, the performance measures in the cost functional can be based on quantities throughout the domain, such as a target velocity distribution as in Gunzburger & Manservisi (1999, 2000), where it is referred to as velocity tracking, or only at the boundaries, such as the wall shear stress. For example, the target velocity or shear stress could be set to their corresponding values in an unseparated boundary layer, *i.e.* without the action of the adverse pressure gradient. Moreover, the domain- or boundary-based performance measure may be applied in one of two ways in the context of optimal control. It may be applied over a specified time interval $0 \leq t \leq T$, or it may be applied at a terminal time $t = T$, which would lead to the control that should be applied over the time interval

$0 \le t \le T$ in order to minimize the cost functional at $t = T$. Either of the domain- or boundary-based control approaches, *i.e.* actuation methods, may be combined with either of the performance measures to provide an optimal control methodology.

To illustrate the approach, let us consider *domain*-based control with a *domain*-based performance measure. Additional cost functionals may be considered by combining a domain-based performance measure with a boundary-based penalty function, or by combining a boundary-based performance measure with either a domain- or boundary-based penalty function as discussed previously. In the domain-domain case shown here, the control variable is the body force $X(x, y, t)$ throughout the boundary layer, and $u_w(x, t) = v_w(x, t) = 0$. The performance measure consists of minimizing the difference between the actual streamwise velocity $u(x, y, t)$ and a prescribed target velocity $\bar{u}(x, y, t)$. In this case the target velocity may be the Rayleigh solution for a diffusing boundary layer, *i.e.* the solution with no adverse pressure gradient acting on the boundary layer. Therefore, we seek the body force distribution $X(x, y, t)$ that will most closely produce the desired target streamwise velocity distribution $\bar{u}(x, y, t)$ throughout the domain (performance measure) while minimizing the total energy input required (penalty function). Optimal control is then defined as the velocity distribution $u(x, y, t)$ and body force distribution $X(x, y, t)$ that minimizes the following cost functional over a time interval $0 \le t \le T$

$$J^*[u^*, v^*, X^*] = \frac{1}{2}\int_0^{T^*}\int_0^{\delta_{bl}}\int_{-\infty}^{\infty}\left[c_w^2\rho(u^* - \bar{u}^*)^2 + d\,(\rho L X^*)^2\right] dx^* dy^* dt^*, \qquad (9)$$

where δ_{bl} is the boundary-layer thickness. The weight coefficient c_w^2 sets the relative weights of the two terms in the cost functional. The first term, *i.e.* performance measure, represents *control effectiveness* and minimizes the differential kinetic energy of the velocity profile. The second term, *i.e.* penalty function, represents *control minimization* and seeks to minimize one half of the square of the energy introduced by the body-force input required to accomplish the control. Note that in an actual flow the performance measure would be based on the measurements from the sensors, and the penalty function corresponds to the output from the actuators. Setting $c_w^2 = 0$ corresponds to the no-control case, *i.e.* $X(x, y, t) = 0$, and increasing c_w^2 increases the importance of the performance measure relative to the penalty function. The coefficient d is included in order to maintain dimensional consistency between the two terms in the cost functional. Note that both terms in the integrand are squared as it is the magnitude of each that is to be minimized; this also allows for the performance measure and penalty function to be interpreted as energies. Non-dimensionalizing and scaling according to equation (4) along with the dimensional coefficient $d = 1/\rho U^2$ gives the non-dimensional cost functional

$$J[u, v, X] = \frac{J^*}{\rho H^3 U Re^{-1/2}} = \frac{1}{2}\int_0^{T}\int_0^{\infty}\int_{-\infty}^{\infty}\left[c_w^2(u - \bar{u})^2 + X^2\right] dx dy dt. \qquad (10)$$

Determination of the optimal control strategy consists of minimizing the cost functional (10) (with specified c_w^2) subject to the constraint that the boundary-layer equations (5) are satisfied. The constraints are included in the cost functional using Lagrange multipliers, and we take the variation of the functional and set it equal to zero, *i.e.* $\delta J[u, v, X] = 0$. This leads to the control, *i.e.* adjoint, equations

$$\frac{\partial X}{\partial t} + u\frac{\partial X}{\partial x} + v\frac{\partial X}{\partial y} + \frac{\partial v}{\partial y}X + \frac{\partial \Lambda}{\partial x} = -\frac{\partial^2 X}{\partial y^2} + c_w^2(u - \bar{u}), \quad \frac{\partial \Lambda}{\partial y} = X\frac{\partial u}{\partial y}, \quad (11)$$

where $\Lambda(x, y, t)$ is a Lagrange multiplier (the other Lagrange multiplier leads to $\lambda = X$). The corresponding initial and boundary conditions are

$$X(x, y, T) = 0, \quad X(x, 0, t) = 0, \quad X(x, \infty, t) = 0, \quad \Lambda(x, \infty, t) = 0. \tag{12}$$

From the last condition we can integrate the second of equations (11) from the edge of the boundary layer toward the wall as follows

$$\Lambda(x, y, t) = \int_{\infty}^{y} X \frac{\partial u}{\partial \hat{y}} d\hat{y} \tag{13}$$

to obtain the adjoint variable $\Lambda(x, y, t)$.

The cost functional (10), and the corresponding control equations (11), represent the *optimal* control case. The control equation (11) for $X(x, y, t)$ and (13) for $\Lambda(x, y, t)$ are coupled with the boundary-layer equations (5) for $u(x, y, t)$ and $v(x, y, t)$. Note that the control equation in (11) is a convection-diffusion equation for the body force $X(x, y, t)$ that must be solved backward in time due to the signs of the unsteady and diffusion terms. This backward time integration is consistent with the initial condition for the control equation in (12). Therefore, the optimal control equations must be solved backward in time starting from $t = T$, while the boundary-layer equations are solved forward in time starting from $t = 0$. Because they are coupled, repeated numerical time integrations of the boundary-layer and control equations are require in order to obtain the converged optimal solution for the control variable, in this case $X(x, y, t)$, and the corresponding boundary layer solution $u(x, y, t)$ and $v(x, y, t)$. In practice, the solution to the optimal control problem provides an upper bound on the potential for flow control in a given application.

Because solution of the optimal control problem described above is very expensive computationally, here we consider the *sub-optimal* case in which the control equation is solved in a quasi-steady manner (see, for example, Min & Choi 1999). In the quasi-steady context the unsteady term in equation (11) is eliminated, but the control variables $X(x, y, t)$ and $\Lambda(x, y, t)$ remain time dependent as $[u(x, y, t) - \bar{u}(x, y, t)]$, which is the forcing term in the control equation, is time dependent. This corresponds to applying the cost functional at each time t, rather than over a time interval $0 \leq t \leq T$.

3. Numerical Results

3.1. No-Control Case

Using the same combined Eulerian and Lagrangian approach as in Cassel (2000), results are shown in this section for the unsteady boundary-layer equations with no control, *i.e.* $c_w^2 = 0$ and $X(x, y, t) = 0$. These results illustrate the unsteady separation process that is to be suppressed, and they provide the baseline for comparison with the sub-optimal control results in the next section.

For a case with $\alpha = 0.10$, *i.e.* ten percent of the incoming flow is diverted through the suction slot, Figure 5 shows the instantaneous streamlines at three successive times. The suction slot in the upper wall, which is centered at $x = 0$ and has width $b = 0.5$, produces an adverse pressure gradient that acts on the boundary layer along the lower wall, which is at $y = 0$. As shown in figure 5(a), the adverse pressure gradient leads to formation of a recirculation region. This recirculation region grows in size normal to the wall and causes the flow in the outer portion of the boundary layer to change directions abruptly in order to pass over it as shown in figure 5(b). Intensification of the flow normal to the wall on the upstream, *i.e.* left, side of the recirculation region eventually results in a non-interactive boundary-layer singularity as in Van Dommelen (1980) and Peridier *et al.* (1991). This is shown in figure 5(c) at the singularity time $t = t_s = 16.35$, at which time the displacement thickness and normal velocity at the outer edge of the boundary layer become singular. Increasing the suction ratio α accelerates the unsteady separation process such that the singularity occurs at earlier times.

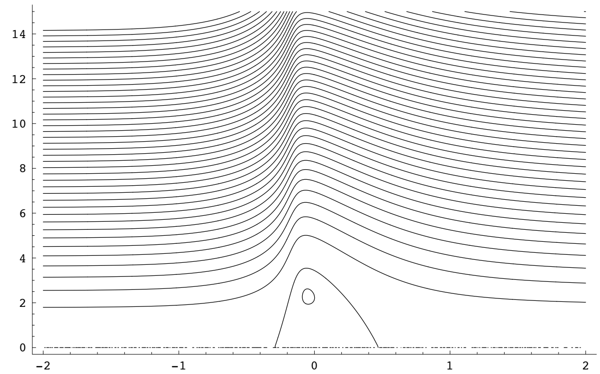

(a) $t = 14.00$.

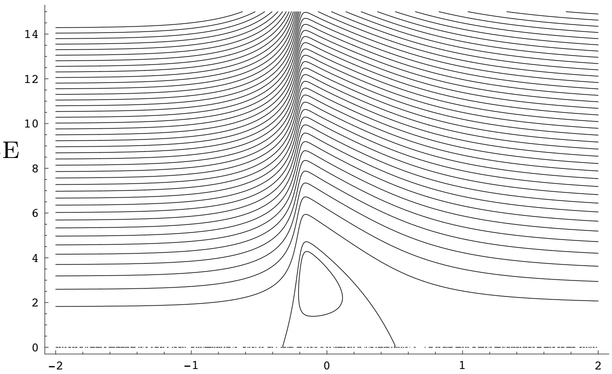

(b) $t = 15.00$.

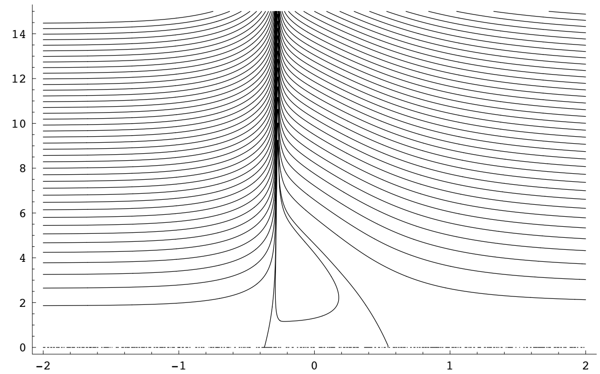

(c) $t = t_s = 16.35$.

Figure 5. Boundary-layer solution for $\alpha = 0.10$.

3.2. Sub-Optimal Control Case

Numerical results for the quasi-steady, sub-optimal control case will be shown during the conference.

4. Conclusions

Sub-optimal control of the unsteady separation that occurs along the lower wall of a channel with a suction slot along the upper wall is considered using the unsteady boundary-layer equations as the state equations. Various combinations of domain- and boundary-based performance measures and penalty functions are considered with respect to their ability to suppress the unsteady separation process. The sub-optimal approach consists of solving the unsteady boundary-layer equation along with the quasi-steady control equation, *i.e.* the control equation must be satisfied at each time during the evolution of the unsteady boundary-layer.

Although the sub-optimal control approach considered here would be expected to result in a control scenario that requires more energy input than the optimal control approach, it provides considerable insight into the feasibility of the various control methodologies. The four possible approaches are 1) domain-based control with domain-based performance measure, 2) domain-based control with boundary-based performance measure, 3) boundary-based control with domain-based performance measure, and 4) boundary-based control with boundary-based performance measure. The sub-optimal control results obtained here, which can be obtained much more efficiently than the optimal solution, will guide future investigations of the optimal control approach by suggesting which combinations of performance measure and penalty function are most effective in suppressing unsteady separation.

Acknowledgements

This work was partially funded by the EPSRC. KWC would like to thank A. Ruban and J. Gajjar for hosting him during extended visits to the University of Manchester.

References

1. Alam, M. & Sandham, N. D., Direct numerical simulation of 'short' laminar separation bubbles with turbulent reattachment. *J. Fluid Mech.*, **410** (2000) 1–28.
2. Alrefai, M. and Acharya, M., Controlled leading-edge suction for management of unsteady separation over pitching airfoils. *AIAA J.*, **34** (1996) 2327–2336.
3. Bewley, T, R., Moin, P. & Temam, R., DNS-based predictive control of turbulence: an optimal benchmark for feedback algorithms. *J. Fluid Mech.*, **447** (2001) 179–225.
4. Cassel, K. W., A comparison of Navier-Stokes solutions with the theoretical description of unsteady separation. *Phil. Trans. R. Soc. Lond. A*, **358** (2000) 3207–3227.
5. Cassel, K. W., The effect of convective heat transfer on unsteady boundary-layer separation.*J. Fluid Mech.*, **428** (2001) 107–131.
6. Degani, A. T., Walker, J. D. A. & Smith, F. T., Unsteady separation past moving surfaces. *J. Fluid Mech.*, **375** (1998) 1–38.
7. Doligalski, T. L., Smith, C. R. & Walker, J. D. A., Vortex interactions with walls. *Ann. Rev. Fluid Mech.*, **26** (1994) 573–616.
8. Gunzburger, M. D., & Manservisi, S., The velocity tracking problem for Navier Stokes flows with bounded distribution controls. *SIAM J. Control Optimization*, **37** (1999) 1913–1945.
9. Gunzburger, M. D., & Manservisi, S., The velocity tracking problem for Navier Stokes flows with boundary controls. *SIAM J. Control Optimization*, **39** (2000) 594–634.
10. Min, C., & Choi, H., Suboptimal feedback control of vortex shedding at low Reynolds numbers. *J. Fluid Mech.*, **401** (1999) 123–156.
11. Obabko, A. V. & Cassel, K. W., Detachment of the dynamic-stall vortex above a moving surface. *AIAA J.*, **40** (9) (2002a) 1811–1822.
12. Obabko, A. V. & Cassel, K. W., Navier-Stokes solutions of unsteady separation induced by a vortex. *J. Fluid Mech.*, **465** (2002b) 99–130.
13. Pauley, L. L., Moin, P. & Reynolds, W. C., The structure of two-dimensional separation. *J. Fluid Mech.*, **220** (1990) 397–411.
14. Peridier, V. J., Smith, F. T. & Walker, J. D. A., Vortex-induced boundary-layer separation. Part 1. The unsteady limit problem $Re \to \infty$. *J. Fluid Mech.*, **232** (1991) 99–131.
15. Van Dommelen, L. L. & Shen, S. F., The spontaneous generation of the singularity in a separating laminar boundary layer. *J. Comput. Phys.* **38** (1980) 125–140.